Novel Benzothiazole Derivatives: Synthesis, Anticancer Activity, Density Function Theory (DFT) Study, and ADMET Prediction

Layla Jasim Abbas[1*] and Kawkab Ali Hussein[2]

[1]*Department of Chemistry, College of Science, University of Basrah, Basrah PO BOX 781, Iraq*

[2]*Department of Chemistry, College of Education for Pure Sciences, University of Basrah, Basrah PO BOX 781, Iraq*

* ***Corresponding author:***

tel: +964-7765050701
email: layla.abbas@uobasrah.edu

Received: May 1, 2024
Accepted: July 29, 2024

DOI: 10.22146/ijc.95838

Abstract: *Benzothiazole is an amazing small molecule involved in many applications in industrial and pharmaceutical industries to prepare many candidate compounds as effective drugs. In this study, we presented some derivatives of this compound that were prepared easily and quickly with the help of microwaves to minimize time, energy, and finances. The compounds' cytotoxicity against the two cell lines SK-GT-4 and AMGM5 was examined. The cytotoxic effect of each compound at different concentrations was measured using the MTT assay. Compounds* ***B1*** *and* ***B2*** *had a high* IC_{50} *value and good growth inhibition activity against the AMGM5 cell line. According to* in silico *absorption, distribution, metabolism, and excretion analysis (ADME) prediction studies, the compounds* ***B1****,* ***B2****, and* ***B3*** *met Lipinski and were drug-like in most physicochemical parameters. Despite some violations, generally favorable pharmacokinetic properties. It is also assumed that it can potentially become a drug candidate in the future. Various electronic parameters were examined using DFT/WB97XD/6-31++G(d,p), and studies were conducted to support the experimental findings. To estimate the binding modes of compounds* ***B1*** *and* ***B5****, we also performed* in silico *molecular docking studies.*

Keywords: *ADME prediction; anticancer; benzothiazole; DFT; microwave radiation assistance*

■ INTRODUCTION

Benzothiazole moiety is reported to have pharmacological properties [1-3], including anticancer, anti-HIV, antiviral, antioxidant, anti-inflammatory, and others [4]. Apoptosis (cell death) and inflammation are known to be caused by the enzyme c-Jun N-terminal kinase (JNK), which is inhibited by the compound (benzothiazole-2yl)acetonitrile. Research on the structure-activity relationship (SAR) of (benzothiazole-2yl)acetonitrile compounds demonstrated that benzothiazole-2-pyridinyl scaffolds are critical for the JNK inhibition activity. To obtain (benzothiazole-2yl)-2-(2-substituted pyrimidine-4yl)acetic acids, the nitrile group was hydrolyzed in acid and the anti-inflammatory capabilities were then examined [5].

The 4-benzothiazol-2-yl-phenylamine derivatives were tested towards MCF-7 and MDA-231 cell lines for human breast cancer. These compounds showed strong anticancer efficacy. To investigate potential interactions between these molecules and the epidermal growth factor receptor (EGFR), which is highly expressed in breast cancer. The synthesized compounds were docked into the EGFR [6]. About sixty human carcinoma cell lines obtained from nine neoplastic disorders were evaluated for their potent anticancer *in vitro* activity using *N*-[4-(benzothiazole-2-yl)phenyl]acetamide derivatives containing various heterocyclic ring structures [7]. Chalcones-benzothiazole compounds' antiproliferative and antioxidant activities on PANC-1 pancreatic cancer cells were investigated [8]. In the one-dose screening panel, thirty-five benzothiazole derivative compounds coupled to various heterocyclic components were created by various chemical processes, and their potential *in situ* antitumor activity was evaluated against

sixty human cancer cell lines. Only two compounds stood out for their strong activity in the whole panel assay with five doses and were chosen for further analysis [9].

Benzothiazole derivatives were synthesized, and their functional activity and binding affinity to CB1 and CB2 receptors were assessed [10]. Mishra and co-workers [11] synthesized two Schiff bases derived from benzothiazole. They complexed them with lanthanide and investigated the anti-bacterial activity against bacteria *Staphylococcus aureus* (MTCC 1144) and *Propionibacterium acnes* (MTCC 1951). Benzothiazole Schiff bases are synthesized by condensing various aromatic aldehydes with 4,6-difluoro-2-amino benzothiazole and screened for antimicrobial activity [12]. Benzothiazole derivatives were synthesized and were evaluated as inhibitors for monoamine oxidases (MAO) enzymes [13]. Thiazole/oxazole substituted benzothiazole derivatives were created and evaluated for their anti-inflammatory, analgesic, ulcerogenic, and free radical scavenging properties [14]. Screening for anticonvulsants using functionalized aryloxadiazole amine and benzothiazole acetamide indoline derivatives was accomplished [15].

It was possible to create phenylacetamide derivatives with the benzothiazole core. The potential of these substances to stop the growth of paraganglioma and pancreatic cancer cell lines was then investigated. Both paraganglioma and pancreatic cancer cells experienced a notable reduction in viability when exposed to the compounds at low doses [16-17]. In the current research, imidazo[2,1-*b*][1,3,4]thiadiazole derivatives containing the benzothiazole group were synthesized and tested for anticancer activity. Theoretical calculations supported the experimental findings. DFT/WB97XD functional with 6-31++G(d,p) basis set was used to optimal structures of the compounds to study the chemical global reagent descriptors (CGRDs), absorption, distribution, metabolism, and excretion analysis (ADME) parameters, and pharmacokinetic properties.

■ EXPERIMENTAL SECTION

Materials

Several chemicals were used in this study, such as 5-bromopyridine-2-carbaldehyde (97%), thiophene-2-carbaldehyde (96%), 4-bromobenzaldehyde (98%), 4-(benzyloxy)benzaldehyde (97%), and 5-(4-bromophenyl)furfural (97%). All chemicals were purchased from Sigma Aldrich without further purification.

Instrumentation

Nuclear magnetic resonance (NMR) spectra were conducted at the University of Basrah's Department of Chemistry in the College of Education for Pure Sciences. The ^{1}H-NMR was recorded using a Bruker Avance NEO 400 (400 MHz) spectrometer. The chemical shift information for each resonance signal is given in terms of parts per million (ppm) relative to tetramethylsilane (TMS) when ^{1}H-NMR spectra are assigned. The College of Pure Sciences at Thi-Qar University used a Bruker/FTIR Tensor 27 spectrophotometer (Japan) to perform measurements of infrared (IR) spectra. Mass spectra (MS) were obtained using a Shimadzu GCMS-QP2010 plus model at Samarah University.

Procedure

Synthesis of the compounds

2-Amino-6-fluorobenzothiazole (I). The compound was synthesized from 4-fluoroaniline (I) as mentioned in the literature [18]. In order to obtain pure pale-yellow needles of the compound, 1:1 aqueous-ethanol was used to recrystallize it. The result has yielded 87% and melting point (m.p.) of 182–185 °C. The compound was used to prepare the Schiff bases without further characterization. The five compounds were made in an environmentally friendly manner by condensation of the benzothiazole amine (I) with the aldehydes (II-VII) in the microwave, according to Scheme 1 (no reagent or catalyst, small amount of solvent, short reaction time, and high output). Crude products were washed with ether first (to remove the aldehyde), then purified using column chromatography (SiO_2 as packing material and ethyl acetate 0–10% in chloroform as eluent).

***N*-((5-bromopyridin-2-yl) methylene)-6-fluorobenzothiazol-2-amine (B1).** 5-Bromopyridine-2-carbaldehyde (0.332 g, 1.785 mmol.) and 6-fluorobenzothiazol-2-amine (0.3 g, 1.784 mmol.) were condensed in the presence of methanol (5 mL) using the

microwave (800 W) for 1 min. The product yield after purification was 0.4 g or 1.191 mmol. The compound is freely soluble in chloroform and DMSO. ^{1}H-NMR (500 MHz, DMSO-d_6) δ: 9.00 (Schiff base proton, s, 1H), 8.70 (d, J = 34.5 Hz, 1H), 8.09 (s, 1H), 7.61 (s, 1H), 7.37 (s, 1H), 7.04 (s, 1H), 6.84 (s, 1H). ^{13}C-NMR (126 MHz, DMSO-d_6) δ: 164.48, 158.40, 156.52, 149.93, 148.64, 139.83, 131.73, 123.37, 119.81, 119.11, 113.11, 112.91, 107.90.

6-Fluoro-*N*-(thiophen-2-ylmethylene)-benzothiazol-2-amine (B2). Thiophene-2-carbaldehyde (0.201 g, 0.17 mL, 1.786 mmol) and 6-fluorobenzothiazol-2-amine (0.3 g, 1.784 mmol) were condensed in the presence of methanol (5 mL) using the microwave (800 W) for 1 min. The product yield after purification was 0.25 g or 0.954 mmol. The compound is freely soluble in chloroform and DMSO. ^{1}H-NMR (500 MHz, DMSO-d_6) δ: 9.31 (Schiff base proton, s, 1H), 8.05 (s, 1H), 8.03–7.93 (m, 2H), 7.89 (s, 1H), 7.33 (d, J = 20.7 Hz, 2H). ^{13}C-NMR (126 MHz, DMSO-d_6) δ: 170.97, 160.12, 148.08, 140.58, 138.44, 135.43, 129.25, 123.76, 115.13, 114.94, 108.97, 108.75.

***N*-(4-bromobenzylidene)-6-fluorobenzothiazol-2-amine (B3).** 4-Bromobenzaldehyde (0.330 g, 1.784 mmol) and 6-fluorobenzothiazol-2-amine (0.300 g, 1.784 mmol) were condensed in the presence of methanol (5 mL) using the microwave (800 W) for 1 min. The product yield after purification was 0.27 g or 0.808 mmol. The compound is freely soluble in chloroform and DMSO. ^{1}H-NMR (400 MHz, $CDCl_3$) δ: 9.01 (Schiff base proton, s, 1H), 7.97–7.83 (m, 3H), 7.68 (t, J = 9.2 Hz, 2H), 7.53 (d, J = 6.1 Hz, 1H), 7.22 (t, J = 9.0 Hz, 1H). ^{13}C-NMR (101 MHz, $CDCl_3$) δ: 164.74, 133.51, 132.47, 131.43, 131.01, 128.40, 124.25, 115.35, 115.11, 113.89, 113.65, 108.21, 107.83, 107.56.

6-Fluoro-*N*-(4-(phenoxymethyl)benzylidene)benzothiazol-2-amine (B4). 4-(Benzyloxy) benzaldehyde (0.380 g, 1.793 mmol) and 6-fluorobenzothiazol-2-amine (0.30 g, 1.784 mmol) were condensed in the presence of methanol (5 mL) using the microwave (800 W) for 1 min. The product yield after purification was 0.45 g or 1.243 mmol. The compound is freely soluble in chloroform and DMSO. ^{1}H-NMR (400 MHz, $CDCl_3$) δ: 8.90 (Schiff base proton, s, 1H), 7.95 (d, J = 8.6 Hz, 2H), 7.87 (dt, J = 10.3, 5.1 Hz, 1H), 7.82 (d, J = 8.6 Hz, 1H), 7.51–7.29 (m, 10H), 7.17 (td, J = 9.0, 2.4 Hz, 1H), 7.06 (d, J = 8.3 Hz, 3H), 5.12 (s, 4H). ^{13}C-NMR (101 MHz, $CDCl_3$) δ: 165.37, 163.76, 135.96, 132.44, 132.05, 130.12, 128.77, 128.38, 127.54, 123.87, 123.78, 119.72, 115.43, 115.17, 114.78, 113.83, 113.59, 108.16, 107.89, 107.56, 70.28.

***N*-((5-(4-bromophenyl) furan-2-yl) methylene)-6-fluorobenzothiazol-2-amine (B5).** 5-(4-Bromophenyl) furfural (0.448 g, 1.784 mmol) and 6-fluorobenzothiazol-2-amine (0.30 g, 1.784 mmol) were condensed in the presence of methanol (5 mL) using the microwave (800 W) for 1 min. The product yield after column chromatography was 0.70 g or 1.750 mmol. The compound is freely soluble in chloroform and DMSO. ^{1}H-NMR (400 MHz, $CDCl_3$) δ: 9.17 (s, Schiff base proton, s, 1H), 7.88 (dd, J = 8.9, 4.9 Hz, 1H), 7.73–7.68 (m, 3H), 7.51 (dd, J = 8.1, 2.5 Hz, 1H), 7.20 (m, J = 8.6, 2.9 Hz, 3H). ^{13}C-NMR (101 MHz, $CDCl_3$) δ: 183.05, 161.45, 159.01, 158.08, 148.22, 141.17, 136.35, 136.20, 135.60, 135.17, 134.11, 128.57, 128.33, 123.93, 123.84, 115.16, 114.92, 113.84, 113.60, 108.14, 107.88, 107.54.

Anticancer activity

Cancer cell lines AMGM5 (cerebral glioblastoma multiforme) [19], and SK-GT-4 cell line (oesophageal adenocarcinoma, CAS 11012007-1VL) were obtained from the IRAQ Biotech Cell Bank Unit in Basrah and kept up with in RPMI-1640 enhanced with 10% Fatal ox-like, 100 unit/mL penicillin, and 100 µg/mL streptomycin. After passage with trypsin-EDTA, the cells were reseeded at 70% confluence twice to three times per week and kept at 37 °C and 5% CO_2 [20].

Cell viability assays

To determine the cytotoxic effect, the microculture tetrazolium (MTT) cell viability assay was performed on 96-well plates. At 1×10^4 cells per well, cell lines were plated [21]. Cells were subjected to test compounds (at different concentrations for each compound) after 24 h or when a confluent monolayer was attained. Cells viability was determined by removing the medium after 72 h of the treatment. Then, 28 µL of a 2 mg/mL MTT solution was added, and the cells were then incubated for 2 h at 37 °C. Following the removal of the MTT solution, the remaining crystals in the wells were solubilized by

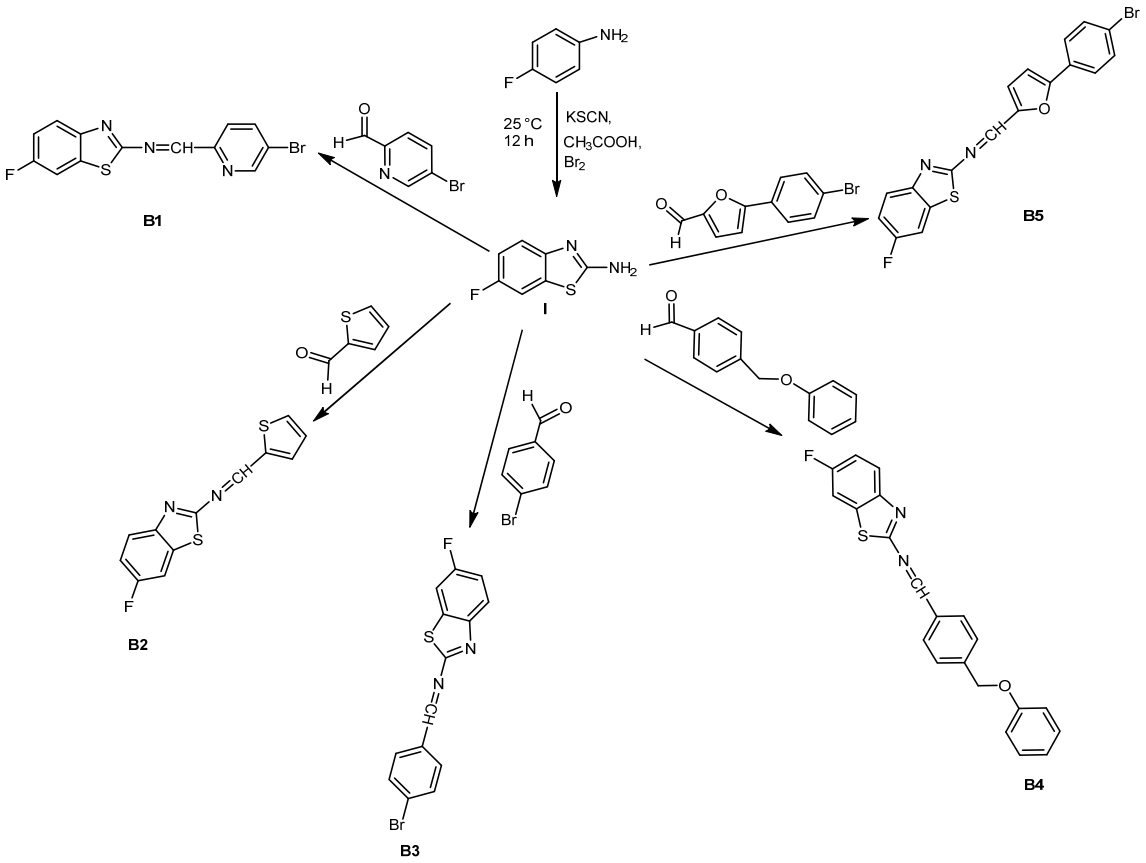

Scheme 1. The preparation route for the synthesized Schiff bases

adding 100 µL of DMSO, which was then incubated at 37 °C for 15 min, as they were shaking [22]. This test was completed in triplicate, and the wavelength of 620 nm was used to evaluate absorbency using a microplate reader. The percentage of cytotoxicity, or the rate at which cell growth was inhibited or the proliferation rate is described in Eq. (1);

$$PR = \frac{B}{A} \times 100 \quad (1)$$

where A is the mean optical density of untreated wells and B is the optical density of treated wells. IR is equal to 100-PR [23].

Computational details

Gaussian 09 program [24] has been employed to estimate the ground-state optimizations of compounds conducted using DFT/WB97XD functional with 6-31++G(d,p) basis set. Optimizing computed geometries has been accomplished using frequency calculations. The fact that all wavenumbers have real values demonstrates that the geometry optimization was successful in quantum chemistry.

ADME prediction

The SwissADME software was utilized to predict molecules' pharmacokinetic and physicochemical parameters based on their molecular structure.

■ RESULTS AND DISCUSSION

4-fluoroaniline compound (I) was synthesized to prepare five Schiff bases (**B1**–**B5**). The five compounds were made environmentally friendly by condensing the benzothiazole amine (I) with five aldehydes (II-VII) in a microwave, according to Scheme 1. Product's identification using IR, GC-MS, ^{1}H, and ^{13}C-NMR spectra were conducted. All compounds' structures were confirmed, as shown in Supplementary Data. The physical properties and molecular formula of the compounds are shown in Table 1.

Table 1. The physical properties of **B1**–**B5** compounds

Compound	Molecular formula	M.wt (g/mol)	Color	Reaction time (min)	Mp. (°C)	Yield (%)
B1	$C_{13}H_7BrFN_3S$	336	Yellow	1	185–188	67
B2	$C_{12}H_7FN_2S_2$	262	Yellow	1	177–180	54
B3	$C_{14}H_8BrFN_2S$	335	Yellow	1	*	45
B4	$C_{21}H_{15}FN_2OS$	362	Yellow	1	72–75	70
B5	$C_{18}H_{10}BrN_2OS$	401	Yellow	1	137–140	98

*not measured

In Vitro Anticancer Assay

Novel benzothiazole derivatives (**B1**–**B5**) that were recently synthesized then were tested for their ability to inhibit the proliferation of two cancer cell lines, AMGM5 and SK-GT-4 cell lines by being treated with various concentrations (125, 250, 500, 750, and 1000 µM) for 72 h of incubation. The antiproliferative activity was evaluated using the MTT colorimetric test as described by the percentage of cell viability and calculated IC_{50} by GraphPad software (Version 8.0.2). Table 2, MTT assay showed that the benzothiazoles (**B1**–**B5**) were examined against the SK-GT-4 cancer cell line. Unfortunately, all these compounds' findings indicated lower toxicity (no detectable cytotoxic action) on all cell lines tested. Compound **B2**, particularly, was more toxic than any other compound. The percentages of cell viability in relation to various chemical concentrations against AMGM5 and SK-GT-4 cell lines are shown in Fig. 1(a-j). While AMGM5 cells were discovered to be more susceptible to the effects of the examined substances **B1**–**B5**, especially compounds **B1** and **B5** exhibited good growth inhibition activity against the AMGM5 cell line with good IC_{50} value, Table 2. Moreover, compounds **B2**, **B3** and **B4** exhibited low toxicity. Compounds' activity and properties of tumor cells may differ due to changes in their chemical structure. These findings show that *in vitro* cell line apoptosis was caused by benzothiazole [25-26].

Table 2. Cytotoxic effects of **B1**–**B5** compounds on the cell lines AMGM5 and SK-GT-4

Compound	IC_{50} (mg/mL)	
	AMGM5	SK-GT-4
B1	461.6	-
B2	-	-
B3	-	-
B4	-	-
B5	332.0	-

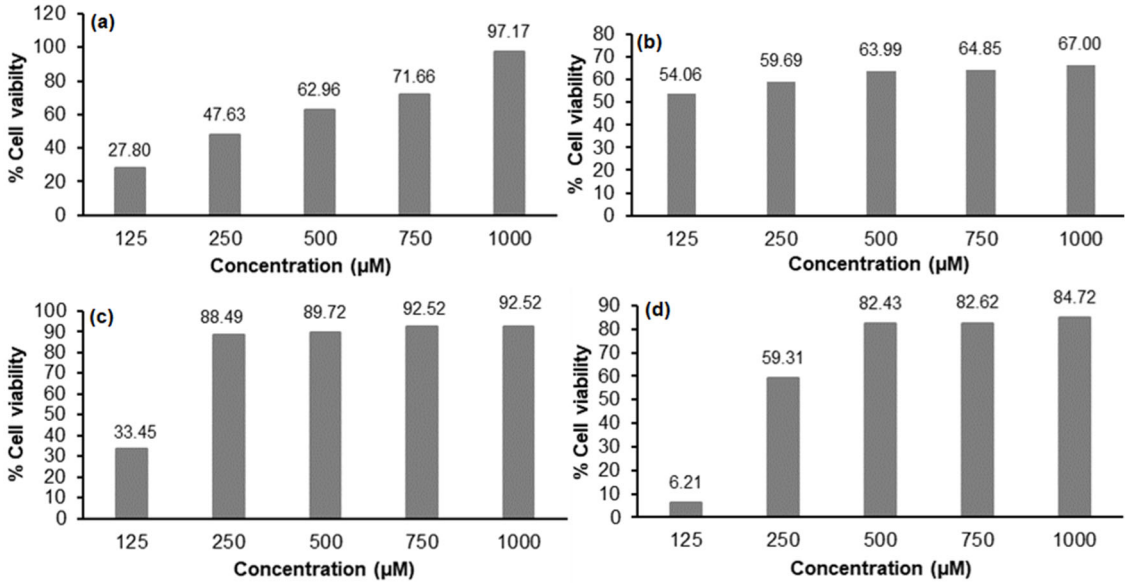

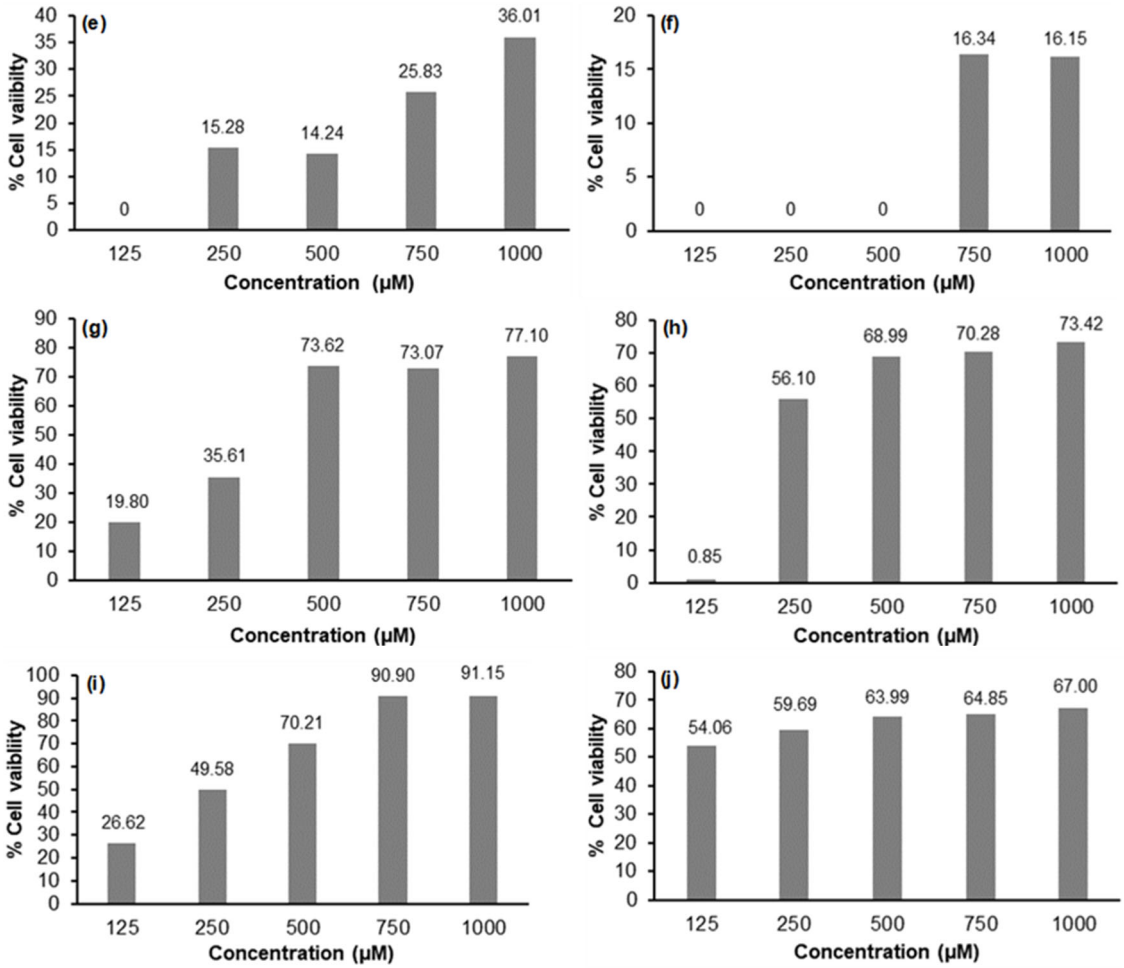

Fig 1. Cell viability of the compound (a, b) **B1**, (c, d) **B2**, (e, f) **B3**, (g, h) **B4**, and (i, j) **B5** against AMGM5 and SK-GT-4 cell lines, respectively, after 72 h of treatment at 37 °C at various doses

In Silico ADME Prediction

SwissADME software was used to anticipate the new compounds' ADME properties. SwissADME offers information on specific fundamental parameters. The goal of the guideline was to develop standards for novel molecular entities in terms of their drug-likeness (Lipinski's rule of five). From Table 3, the molecule's molecular flexibility, which should be less than 10, is measured by the number of rotatable bonds (nRotB). Hydrogen bond acceptor and donor, represented by symbols HBA and HBD, respectively, indicate the nRotB. While donors of H-bonds greater than 5. In addition to Lipinski's parameters [27], other parameters like molar refractivity (MR) measure a compound's volume and its ease of polarization; It varies from 71.15–104.25. To put it another way, the topological polar surface area (TPSA) values were below 140 and ranged from 53.49 to 81.73.

In contrast, lipophilicity behavior is demonstrated by a consensus Log $P_{o/w}$ in the range of 4.11 to 5.52. Compounds **B1**, **B2**, and **B3** are moderately soluble, whereas compounds **B4** and **B5** are poorly soluble. All compounds have a high gastrointestinal absorption rate in humans (GI). Compounds **B2** and **B4** presciently show poor to cross the BBB while other compounds have good BBB. The compounds are non-P-gp substrates; in contrast, the effectiveness of each compound against CYP enzymes varied. The differences between the predictions show that the tested compounds are not thought of as substrates and inhibitors of CYP2D6 inhibitor and CYP3A4. At the same time, it was anticipated that all

Table 3. Calculated ADME properties and pharmacokinetic properties of the compounds

Parameters	Compounds				
	B1	**B2**	**B3**	**B4**	**B5**
Molecular weight	336.18	262.32	335.19	362.42	401.25
No. of rotatable bonds	2	2	2	5	3
No. of HBAs	4	3	3	4	4
No. of HBDs	0	0	0	0	0
Molar refractivity	78.77	71.15	80.97	104.25	98.68
TPSA(A^2)	66.38	81.73	53.49	62.72	66.63
Consensus log $P_{o/w}$	4.11	4.21	4.80	5.47	5.52
Water solubility	Moderate	Moderate	Moderate	Poor	Poor
GI absorption	High	High	High	High	High
BBB permeant	Yes	No	Yes	No	No
P-gp substrate	No	No	No	No	No
CYP1A2 inhibitor	Yes	Yes	Yes	Yes	Yes
CYP2C19 inhibitor	Yes	Yes	Yes	Yes	Yes
CYP2C9 inhibitor	Yes	Yes	Yes	Yes	Yes
CYP2D6 inhibitor	No	No	No	No	No
CYP3A4 inhibitor	No	No	No	No	No
log kp	−5.46	−4.97	−4.94	−4.24	−4.49
Lipinski rule validation	Yes	Yes	Yes	Yes; 1 violation; MLOGP > 4.15	Yes;1 violation; MLOGP > 4.15
Ghose	Yes	Yes	Yes	No; 1 violation; WLOGP > 5.6	No; 1 violation; WLOGP > 5.6
Veber	Yes	Yes	Yes	Yes	Yes
Egan	Yes	Yes	Yes	No; 1 violation; WLOGP > 5.88	No; 1 violation; WLOGP > 5.88
Muegge	Yes	Yes	Yes	No; 1 violation; XLOGP3 > 5	No; 1 violation; XLOGP3 > 5
Bioavailability Score	0.55	0.55	0.55	0.55	0.55
Lead likeness	No;1violation; XLOGP 3 > 3.5	No;1violation; XLOGP 3 > 3.5	No;1violation; XLOGP 3 > 3.5	No; 2 violations; MW > 350 XLOGP3 > 3.5	No; 2 violations; MW > 350 XLOGP3 > 3.5

compounds would inhibit CYP1A2, CYP2C19, and CYP2C9. Skin permeation testing is an important tool for understanding drug delivery into the various skin layers, all compounds showed high values.

The findings demonstrate that synthesized compounds **B1**, **B2**, and **B3** followed Lipinski's rule of five except compounds **B4** and **B5**. Consequently, compounds **B1**, **B2**, and B3 had good drug-like characteristics and reduced potency. In contrast, with high molecular weight (M.wt > 350) and XLOGP3 values, which ought to be greater than 3.5, all compounds displayed two violations in lead likeness, making the drug-likeness profile unfavorable. Additionally, because of their 0.55 bioavailability score, this indicates that they are more drug-like in nature [28].

On the other hand, the substances under investigation have several beneficial ADME characteristics. The compounds' pharmacokinetics, physicochemical characteristics, medicinal chemistry properties and drug-likeness change when their chemical structure is altered [29-31].

Computational Studies

Geometry optimization was used in studying electronic properties depicted as presented in Fig. 2. The energy difference between HOMO and LUMO governs the molecule's kinetic stability, optical polarizability, chemical reactivity, and chemical hardness-softness. Table 4 summarizes the quantum chemical descriptors such as absolute electronegativity, global hardness, and softness.

As shown in Table 4, the E_{HOMO} for compound **B5** is the greatest at −5.9579 eV, while that for compound **B1** is the lowest at −8.339 eV. The E_{LUMO} of compound **B5** is the lowest, at −2.8471 eV, and compound **B4** has the highest, at −0.7415 eV. Molecules with a large energy gap (ΔE) have low chemical reactivity but high kinetic stability due to their rapid electron donation to an acceptor (a low-energy gap molecule is generally more reactive). On the other hand, a high-energy gap molecule is known as a "hard molecule" and is challenging to polarize because the excitation requires greater energy [32]. Compound **B4** (the hard molecule) is the most stable and least reactive, while compound **B5** (the soft molecule) is the most stable and most reactive.

The electronic chemical potential (μ) can be calculated as shown in Eq. (2) [33], to explain the tendency of electrons in an equilibrium system to leave.

$$\mu = \frac{1}{2}(E_{HOMO} + E_{LUMO}) \quad (2)$$

The order of electronic chemical potentials is **B5** > **B4** > **B2** > **B3** > **B1**. The ability of an atom or group of atoms to draw electrons is characterized by a feature known as electronegativity (χ), which may be computed using the formula in Eq. (3) [34].

$$\chi = -\frac{1}{2}(E_{HOMO} + E_{LUMO}) \quad (3)$$

The order of electronegativity is from small to large: **B5** < **B4** < **B2** < **B3** < **B1**. A chemical system's stability and reactivity are related to its chemical hardness, and it demonstrates how hard it is to modify the electron or charge distribution of a molecule [35]. It is calculated by Eq. (4).

Table 4. Chemical global reagent descriptors (CGRDs) for compounds understudy by DFT/WB97XD/6-31++G(d,p)

Compounds	HOMO (eV)	LUMO (eV)	ΔE (eV)	μ (eV)	χ (eV)	H (eV)	S (eV^{-1})	ω
B1	−8.3397	−1.1265	7.2131	−4.7331	4.7331	3.6066	0.2772	3.1057
B2	−8.0725	−0.8968	7.1756	−4.4847	4.4847	3.5878	0.2787	2.8028
B3	−8.2570	−0.9793	7.2776	−4.6182	4.6182	3.6388	0.2748	2.9305
B4	−8.1576	−0.7415	7.4161	−4.4496	4.4495	3.7080	0.2696	2.6696
B5	−5.9579	−2.8471	3.1107	−4.4025	4.4025	1.5554	0.6429	6.2305

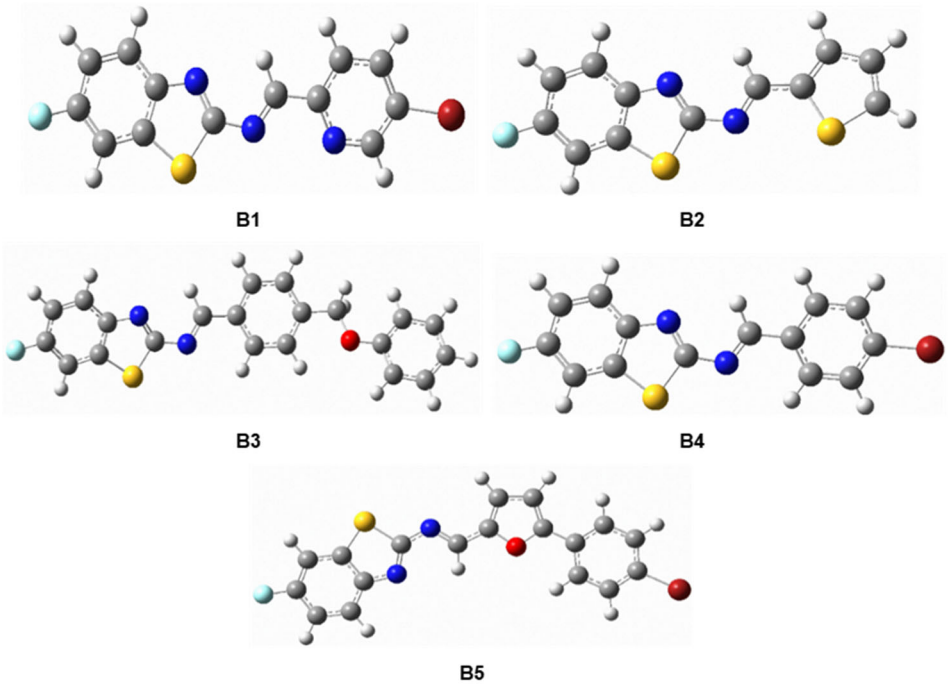

Fig 2. The completely improved benzothiazole compounds at DFT/WB97XD/6-31++G(d,p) level. Red, blue, yellow, light blue, dark grey, and light grey colors indicate Br, N, S, F, C, and H atoms, respectively

$$\eta = \frac{1}{2}(E_{LUMO} - E_{HOMO}) \quad (4)$$

Compound **B5** is found to be less reactive and more stable (harder), while compound **B4** is found to be less stable and more reactive.

$$S = \frac{1}{2\eta} \quad (5)$$

Eq. (5) can be used to calculate softness, which is the opposite of hardness [36]. A softer species (atom or molecule) is usually more polarizable and magnetizable [37]. Compound **B5** is softer and more polarizable, as shown in Table 4, whereas compound **B4** is harder and less polarizable.

The ability of a molecule to acquire electrons is measured by the global electrophilicity index (ω). It can be expressed as indicated in Eq. (6).

$$\omega = \frac{\mu^2}{\eta} \quad (6)$$

The electrophilicity scale can classify organic molecules as strong electrophiles. Strong electrophiles have more than 1.5 eV, while moderate electrophiles have less than 0.8 eV. Marginal electrophiles have less than 0.8 eV. Superelectrophiles have an electrophilicity index greater than 4.0 eV and are highly active in polar reactions [38]. The order of the electrophilicity is as follows: **B5** > **B1** > **B3** > **B2** > **B4**.

Molecular Docking Studies

The main goal was to analyze ligand-protein interactions to understand the mechanism for the highly active compounds action (**B1** and **B5**) on the receptor target. For the AMGM5 cell line, molecular docking was demonstrated using the receptor PDB (ID: 6TE5) [39]. Autodock4 [40] was used for the molecular docking process, and Biovia Discovery Studio Visualizer was used to analyze the results (Table 5). The interactions between compound **B1** and the amino acid residues in the 6TE5 receptor's active site showed that compound **B1** had the best conformational docked pose, with a good fit and binding energy, the amino acid residues that were interacted with the ligand are ARG A:139, GLN A: 474, ALA A: 473, TYR A: 472, LEU A: 489, ASN A: 469, CYS A: 313, LEU A: 185, LEU A: 471, TYR A: 143, PHE A: 182, GLY A: 136, ILE A: 132, and PHE A: 308. Additionally, two hydrogen bonds were formed with TRP A:189 and THR A:140, as shown in Fig. 3(a). Fig. 3(b) shows the optimal pose for the protein-ligand complex in the interaction diagram for compound **B5**. In particular, the interactions with amino acid residues are ARG A: 139, ALA A: 473, TYR A: 472, ASN A: 469, ILE A: 132, PHE A: 308, LEU A: 185, THR A: 315, LEU A: 471, MET A: 186, CYS A: 314, TRP A: 189, PHE A: 182,

Table 5. Mean docked energy for compounds **B1** and **B5** with 6TE5 protein

Compound	Binding (kcal/mol)	Ki (nM)	Final intermolecular energy
B1	−6.93	8310	-7.53
B5	−8.34	770.27	-9.23

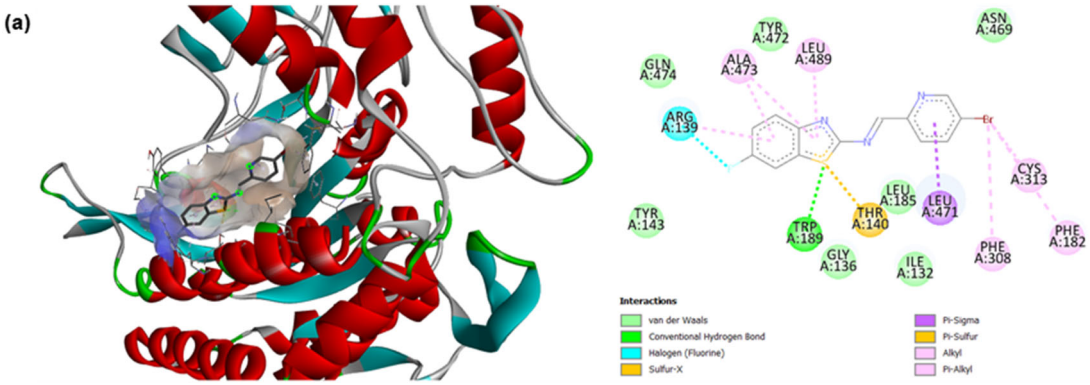

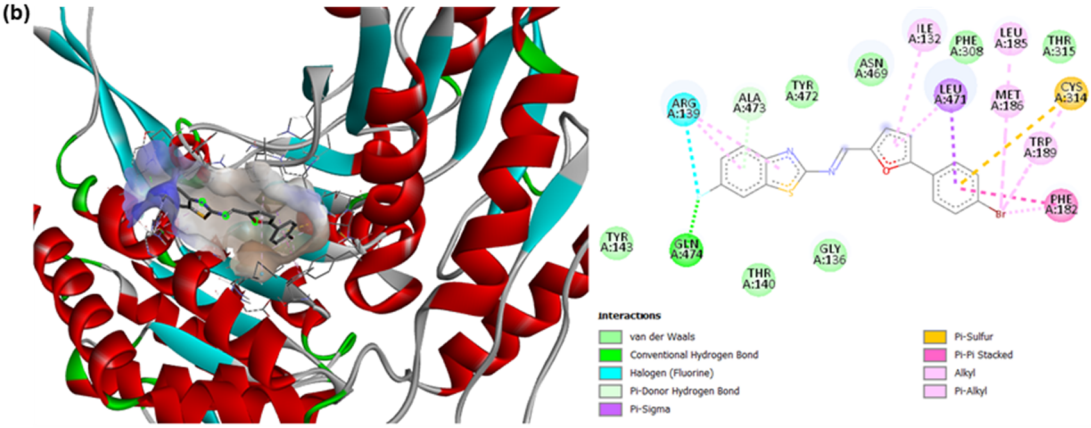

Fig 3. Molecular docking interactions of compounds (a) **B1** and (b) **B5** with 6TE5 receptor

TYR A: 143, GLN A: 475, THR A: 140, and GLY A: 136, are all considered hydrophobic interactions, while two hydrogen bonds with ARG A: 139 and GLN A: 474.

■ CONCLUSION

Five new benzothiazole compounds' synthesis and characterization using IR, NMR, mass techniques, and DFT investigations for evaluation as an anticancer drug have been completed. The antitumor activity of the synthesized compounds was investigated towards AMGM5 and SK-GT-4 cell lines. Regrettably, the MTT assay showed that benzothiazoles **B1**–**B5** examined against the SK-GT-4 cell lines have no activity. Meanwhile, compounds **B1** and **B2** exhibited good growth inhibition activity against the AMGM5 cell line with good IC_{50} value. Moreover, other compound (**B2**, **B3**, and **B4)** exhibited low toxicity. *In silico* ADME Predictions, the compounds **B1**, **B2**, and **B3** met Lipinski. They were drug-like in most physicochemical parameters, according to *in silico* ADME prediction studies, and they had generally favorable pharmacokinetic properties, although they had violations of some kind. It is also assumed that it can become a possible potential future drug candidate. The electronic chemical potentials for molecule **B5** are larger than that for other compounds. The electrophilicity and electronegativity power of compound **B5** can be seen in the calculated values of the global reactivity index. The results of the *in silico* docking studies also showed that compounds **B1** and **B5** have favorable dock scores, binding energies, and affinities for the 6TE5 receptor. As a result, for synthesis, characterization, anticancer activity, molecular docking studies, *in silico* ADME prediction, and molecular geometry, a trial to find new multi-targeted anticancer treatments might be employed in the anticancer medicines and pharmaceutical applications progress.

■ CONFLICT OF INTEREST

There are no conflicts of interest in this paper.

■ AUTHOR CONTRIBUTIONS

Layla Jasim Abbas: provided the chemicals, achieved reactions, purifications of the compounds, and characterization (IR, NMR, and MS), wrote the manuscript, and revised the whole manuscript. Kawkab Ali Hussein: achieved the *in silico* studies.

■ REFERENCES

[1] Rouf, A., and Tanyeli, C., 2015, Bioactive thiazole and benzothiazole derivatives, *Eur. J. Med. Chem.*, 97, 911–927.

[2] Tariq, S., Kamboj, P., and Amir, M., 2019, Therapeutic advancement of benzothiazole derivatives in the last decennial period, *Arch. Pharm.*, 352 (1), 1800170.

[3] Al-Masoudi, N.A., Jafar, N.N.A., Abbas, L.J., Baqir, S.J., and Pannecouque, C., 2011, Synthesis and anti-HIV activity of new benzimidazole, benzothiazole and carbohyrazide derivatives of the anti-inflammatory drug indomethacin, *Z. Naturforsch., B*, 66 (9), 953–960.

[4] Irfan, A., Batool, F., Zahra Naqvi, S.A., Islam, A., Osman, S.M., Nocentini, A., Alissa, S.A., and Supuran, C.T., 2020, Benzothiazole derivatives as anticancer agents, *J. Enzyme Inhib. Med. Chem.*, 35 (1), 265–279.

[5] Doma, A., Kulkarni, R., Garlapati, A., and Krisnha, P.R., 2014, Synthesis and antiinflammatory activity of novel pyrimidino benzothiazole amine derivatives, *Pharmacophore*, 5 (2), 331–342.

[6] Abdelgawad, M.A., Belal, A., Omar, H.A., Hegazy, L., and Rateb, M.E., 2013, Synthesis, anti-breast cancer activity, and molecular modeling of some benzothiazole and benzoxazole derivatives, *Arch. Pharm.*, 346 (7), 534–541.

[7] Yurttaş, L., Tay, F., and Demirayak, Ş., 2015, Synthesis and antitumor activity evaluation of new 2-(4-aminophenyl)benzothiazole derivatives bearing different heterocyclic rings, *J. Enzyme Inhib. Med. Chem.*, 30 (3), 458–465.

[8] Uremis, N., Uremis, M.M., Tolun, F.I., Ceylan, M., Doganer, A., and Kurt, A.H., 2017, Synthesis of 2-substituted benzothiazole derivatives and their *in vitro* anticancer effects and antioxidant activities against pancreatic cancer cells, *Anticancer Res.*, 37 (11), 6381–6389.

[9] Hassan, A.Y., Sarg, M.T., and Hussein, E.M., 2019, Design, synthesis, and anticancer activity of novel benzothiazole analogues, *J. Heterocycl. Chem.*, 56 (4), 1437–1457.

[10] Ghonim, A.E., Ligresti, A., Rabbito, A., Mahmoud, A.M., Di Marzo, V., Osman, N.A., and Abadi, A.H., 2019, Structure-activity relationships of thiazole and benzothiazole derivatives as selective cannabinoid CB2 agonists with *in vivo* anti-inflammatory properties, *Eur. J. Med. Chem.*, 180, 154–170.

[11] Mishra, N., Kumar, K., Pandey, H., Raj Anand, S., Yadav, R., Prakash Srivastava, S., and Pandey, R., 2020, Synthesis, characterization, optical and anti-bacterial properties of benzothiazole Schiff bases and their lanthanide(III) complexes, *J. Saudi Chem. Soc.*, 24 (12), 925–933.

[12] Upadhyay, S.V., Zala, R.V., and Bhatt, K.D., 2020, Synthesis, characterization and biological screening of Schiff bases derived from 4,6-difluoro-2-amino benzothiazole, *Med. Anal. Chem. Int. J.*, 4 (1), 000157.

[13] Acar Çevik, U., Osmaniye, D., Sağlik, B.N., Levent, S., Çavuşoğlu, B.K., Karaduman, A.B., Özkay, Ü.D., Özkay, Y., Kaplancikli, Z.A., and Turan, G., 2020, Synthesis of new benzothiazole derivatives bearing thiadiazole as monoamine oxidase inhibitors, *J. Heterocycl. Chem.*, 57 (5), 2225–2233.

[14] Kumar, G., and Singh, N.P., 2021, Synthesis, anti-inflammatory and analgesic evaluation of thiazole/oxazole substituted benzothiazole derivatives, *Bioorg. Chem.*, 107, 104608.

[15] Nath, R., Shahar Yar, M., Pathania, S., Grover, G., Debnath, B., and Akhtar, M.J., 2021, Synthesis and anticonvulsant evaluation of indoline derivatives of functionalized aryloxadiazole amine and benzothiazole acetamide, *J. Mol. Struct.*, 1228, 129742.

[16] Amoroso, R., De Lellis, L., Florio, R., Moreno, N., Agamennone, M., De Filippis, B., Giampietro, L., Maccallini, C., Fernández, I., Recio, R., Cama, A., Fantacuzzi, M., and Ammazzalorso, A., 2022, Benzothiazole derivatives endowed with antiproliferative activity in paraganglioma and pancreatic cancer cells: Structure–activity relationship studies and target prediction analysis, *Pharmaceuticals*, 15 (8), 937.

[17] Er, M., Özer, A., Direkel, Ş., Karakurt, T., and Tahtaci, H., 2019, Novel substituted benzothiazole and imidazo[2,1-*b*][1,3,4]thiadiazole derivatives: Synthesis, characterization, molecular docking study, and investigation of their *in vitro* antileishmanial and antibacterial activities, *J. Mol. Struct.*, 1194, 284–296.

[18] Matsui, M., Kamino, Y., Hayashi, M., Funabiki, K., Shibata, K., Muramatsu, H., Abe, Y., and Kaneko, M., 1998, Fluorine-containing benzothiazolyl bisazo dyes-their application to guest-host liquid crystal displays, *Liq. Cryst.*, 25 (2), 235–240.

[19] Abdulghany, Z.S., and Mahmood, N.A., 2023, Expression of MAO gene in both starved and non-starved glioblastoma cancer cell line, *Iraqi J. Cancer Med. Genet.*, 16 (1), 21–25.

[20] Al-Ali, A.A.A., Alsalami, K.A.S., and Athbi, A.M., 2022, Cytotoxic effects of CeO_2 NPs and β-carotene and their ability to induce apoptosis in human breast normal and cancer cell lines, *Iraqi J. Sci.*, 63 (3), 923–937.

[21] Falih, S.M.J., Al-Saray, S.T., Alfaris, A.A., and Al-Ali, A.A.A., 2022, The synergistic effect of eucalyptus oil and retinoic acid on human esophagus cancer cell line SK-GT-4, *Egypt. J. Med. Hum. Genet.*, 23 (1), 70.

[22] Al-Shammari, A.M., Al-Esmaeel, W.N., Al Ali, A.A.A., Hassan, A.A., and Ahmed, A.A., 2019, Enhancement of oncolytic activity of Newcastle disease virus through combination with retinoic acid against digestive system malignancies, *Mol. Ther.*, 27 (4), 126–127.

[23] Freshney, R.I., 2010, *Culture of Animal Cell: A Manual of Basic Technique and Specialized Applications*, John Wiley & Sons, Inc., Hoboken, New Jersey, US.

[24] Frisch, M.J., Trucks, G.W., Schlegel, H.B., Scuseria, G.E., Robb, M.A., Cheeseman, J.R., Scalmani, G., Barone, V., Petersson, G.A., Nakatsuji, H., Li, X., Caricato, M., Marenich, A.V., Bloino, J., Janesko, B.G., Gomperts, R., Mennucci, B., Hratchian, H.P., Ortiz, J.V., Izmaylov, A.F., Sonnenberg, J.L., Williams-Young, D., Ding, F., Lipparini, F., Egidi, F., Goings, J., Peng, B., Petrone, A., Henderson, T., Ranasinghe, D., Zakrzewski, V.G., Gao, J., Rega, N., Zheng, G., Liang, W., Hada, M., Ehara, M., Toyota, K., Fukuda, R., Hasegawa, J., Ishida, M., Nakajima, T., Honda, Y., Kitao, O., Nakai, H., Vreven, T., Throssell, K., Montgomery, J.A., Jr., Peralta, J.E., Ogliaro, F., Bearpark, M.J., Heyd, J.J., Brothers, E.N., Kudin, K.N., Staroverov, V.N., Keith, T.A., Kobayashi, R., Normand, J., Raghavachari, K., Rendell, A.P., Burant, J.C., Iyengar, S.S., Tomasi, J., Cossi, M., Millam, J.M., Klene, M., Adamo, C., Cammi, R., Ochterski, J.W., Martin, R.L., Morokuma, K., Farkas, O., Foresman, J.B., and Fox, D.J., 2009, *Gaussian 09 Revision B.01*, Gaussian, Inc., Wallingford, CT.

[25] Kadhim, Z.A., Sulaiman, G.M., Al-Shammari, A.M., Khan, R.A., Al Rugaie, O., and Mohammed, H.A., 2022, Oncolytic Newcastle disease virus co-delivered with modified PLGA nanoparticles encapsulating temozolomide against glioblastoma cells: Developing an effective treatment strategy, *Molecules*, 27 (18), 5757.

[26] Song, S., Xie, M., Scott, A.W., Jin, J., Ma, L., Dong, X., Skinner, H.D., Johnson, R.L., Ding, S., and Ajani, J.A., 2018, A novel YAP1 inhibitor targets CSC-enriched radiation-resistant cells and exerts strong antitumor activity in esophageal adenocarcinoma, *Mol. Cancer Ther.*, 17 (2), 443–454.

[27] Azzam, R.A., Elboshi, H.A., and Elgemeie, G.H., 2022, Synthesis, physicochemical properties and molecular docking of new benzothiazole derivatives as antimicrobial agents targeting DHPS enzyme, *Antibiotics*, 11 (12), 1799.

[28] Abdullahi, S.H., Moin, A.T., Uzairu, A., Umar, A.B., Ibrahim, M.T., Usman, M.T., Nawal, N., Bayil, I., and Zubair, T., 2024, Molecular docking studies of some benzoxazole and benzothiazole derivatives as VEGFR-2 target inhibitors: *In silico* design, MD simulation, pharmacokinetics and DFT studies, *Intell. Pharm.*, 2 (2), 232–250.

[29] Chinnamanyakar, R., and Ramanathan, E.M., 2021, Anti-cancer and antimicrobial activity, *in-silico* adme and docking studies of biphenyl pyrazoline derivatives, *Biointerface Res. Appl. Chem.*, 11 (1), 8266–8282.

[30] Uslu, H., Koparir, P., Sarac, K., and Karatepe, A., 2021, ADME predictions and molecular docking study of some compounds and drugs as potential inhibitors of COVID-19 main protease: A virtual study as comparison of computational results, *Med. Sci.*, 10 (1), 18–30.

[31] Roman, D.L., Roman, M., Som, C., Schmutz, M., Hernandez, E., Wick, P., Casalini, T., Perale, G., Ostafe, V., and Isvoran, A., 2019, Computational assessment of the pharmacological profiles of degradation products of chitosan, *Front. Bioeng. Biotechnol.*, 7, 00214.

[32] Miar, M., Shiroudi, A., Pourshamsian, K., Oliaey, A.R., and Hatamjafari, F., 2021, Theoretical investigations on the HOMO–LUMO gap and global reactivity descriptor studies, natural bond

orbital, and nucleus-independent chemical shifts analyses of 3-phenylbenzo[d]thiazole-2(3*H*)-imine and its para-substituted derivatives: Solvent and subs, *J. Chem. Res.*, 45 (1-2), 147–158.

[33] Pegu, D., Deb, J., Van Alsenoy, C., and Sarkar, U., 2017, Theoretical investigation of electronic, vibrational, and nonlinear optical properties of 4-fluoro-4-hydroxybenzophenone, *Spectrosc. Lett.*, 50 (4), 232–243.

[34] Spirtovic-Halilovic, S., Salihović, M., Džudžević-Čančar, H., Trifunović, S., Roca, S., Softić, D., and Završnik, D., 2014, DFT study and microbiology of some coumarin-based compounds containing a chalcone moiety, *J. Serb. Chem. Soc.*, 79 (4), 435–443.

[35] Hilal, C., Önal, M., and Mert, M.E., 2021, Detonation parameters of the pentaerythritol tetranitrate and some structures descriptors in different solvents - Computational study, *DUBITED*, 9 (4), 1227–1241.

[36] Lopachin, R.M., and Gavin, T., 2014, Molecular mechanisms of aldehyde toxicity: A chemical perspective, *Chem. Res. Toxicol.*, 27 (7), 1081–1091.

[37] Jupp, A.R., Johnstone, T.C., and Stephan, D.W., 2018, The global electrophilicity index as a metric for Lewis acidity, *Dalton Trans.*, 47 (20), 7029–7035.

[38] Domingo, L.R., Ríos-Gutiérrez, M., and Pérez, P., 2016, Applications of the conceptual density functional theory indices to organic chemistry reactivity, *Molecules*, 21 (6), 748.

[39] Quattrini, L., Gelardi, E.L.M., Coviello, V., Sartini, S., Ferraris, D.M., Mori, M., Nakano, I., Garavaglia, S., and La Motta, C., 2020, Imidazo[1,2-a]pyridine derivatives as aldehyde dehydrogenase inhibitors: Novel chemotypes to target glioblastoma stem cells, *J. Med. Chem.*, 63 (9), 4603–4616.

[40] Morris, G.M., Huey, R., Lindstrom, W., Sanner, M.F., Belew, R.K., Goodsell, D.S., and Olson, A.J., 2009, AutoDock4 and AutoDockTools4: Automated docking with selective receptor flexibility, *J. Comput. Chem.*, 30 (16), 2785–2791.